

Impact of quantum entanglement on spectrum of cosmological fluctuations

Sugumi Kanno

*Laboratory for Quantum Gravity & Strings and Astrophysics, Cosmology & Gravity Center,
Department of Mathematics & Applied Mathematics, University of Cape Town,
Private Bag, Rondebosch 7701, South Africa*

Abstract

We investigate the effect of entanglement between two causally separated open charts in de Sitter space on the spectrum of vacuum fluctuations. We consider a free massive scalar field, and construct the reduced density matrix by tracing out the vacuum state for one of the open charts, as recently derived by Maldacena and Pimentel. We formulate the mean-square vacuum fluctuations by using the reduced density matrix and show that the scale invariant spectrum of massless scalar field is realized on small scales. On the other hand, we find that the quantum entanglement affects the shape of the spectrum on large scales comparable to or greater than the curvature radius.

Contents

1	Introduction	1
2	Spectrum of quantum fluctuations in the open chart	2
2.1	Mode functions in the open chart	3
2.2	Spectrum in the L region	6
2.3	Vacuum fluctuations after horizon exit	6
2.4	Wavenumber dependence	7
3	Spectrum of quantum fluctuations using the reduced density matrix	8
3.1	A review on the reduced density matrix	8
3.2	Spectrum of vacuum fluctuations	11
3.3	Spectrum in the L region	12
3.4	Vacuum fluctuations after horizon exit	13
3.5	Wavenumber dependence	14
4	Possible observable signatures	14
4.1	Non-entangled state	15
4.2	Spectra at long wavelengths	16
5	Summary and discussion	17

1 Introduction

Quantum entanglement is one of the most fundamental and fascinating features of quantum mechanics. The most mysterious aspect of quantum entanglement would be to affect the outcome of local measurements instantaneously beyond the lightcone once a local measurement is performed. There are many phenomena in which quantum entanglement may play a role, including the bubble nucleation [1]. Recent studies of the bubble nucleation problem infer that observer frames will be strongly correlated to each other when they observe the nucleation frame [2, 3, 4].

The entanglement entropy as a suitable measure of entanglement of a quantum system has been developed in condensed matter physics, quantum information and high energy physics. Especially, the entanglement entropy has now been established as a useful tool in quantum field theory to characterize the nature of long range correlations.

Even so, however, the explicit calculation of the entanglement entropy in quantum field theories had not been an easy task until Ryu and Takayanagi proposed a method of calcu-

lating the entanglement entropy of a strongly coupled quantum field theory with its gravity dual using holographic techniques [5]. Their formula has passed many consistency checks and proven to be extremely powerful [6].

Following a great deal of attention paid to the success, Maldacena and Pimentel developed an explicit method to calculate the entanglement entropy in a quantum field theory in the Bunch-Davies vacuum of de Sitter space and discussed the gravitational dual of this theory and its holographic interpretation [7]. The method is also extended to α -vacua in [8, 9]

Based on these developments that enable us to calculate long range correlations explicitly, it would be interesting to apply this to cosmology now. We expect that the entanglement could exist beyond the Hubble horizon because de Sitter expansion eventually separates off a pair of particles created within a causally connected, Hubble horizon size region. It may be possible to investigate whether a universe entangled with our own universe exists within the multiverse framework. Such a scenario may be observable through the cosmic microwave background radiation (CMB).

In this paper, we investigate the effect of quantum entanglement on the spectrum of vacuum fluctuations in de Sitter space by using a reduced density matrix in the open chart derived by Maldacena and Pimentel as a first step of application to cosmology. It is known that the inside of a nucleated bubble looks like an open universe [1], so this formulation will be suitable for the multiverse framework and also for open inflation directly. The open inflation models are discussed extensively in [10, 11, 12, 13, 14, 15].

The paper is organized as follows. In section 2, we review the spectrum of quantum fluctuations in the open chart. In section 3, we review the method to derive the reduced density matrix developed by Maldacena and Pimentel with some comments relevant to its application to cosmology. Then we discuss the spectrum of quantum fluctuations using the reduced density matrix. We show the scale invariant spectrum is realized. In section 4, we find the effect of the entanglement appears in the spectrum at large wavelengths comparable to the curvature radius. Our results are summarized and discussed in section 5.

2 Spectrum of quantum fluctuations in the open chart

In this section, we review the spectrum of vacuum fluctuations in the open chart as a preparation for later sections. The Penrose diagram of the open chart is given in Figure 1, where the two time slices A and B represent, respectively, a time slice in each open chart R and L at sufficiently late time in future.

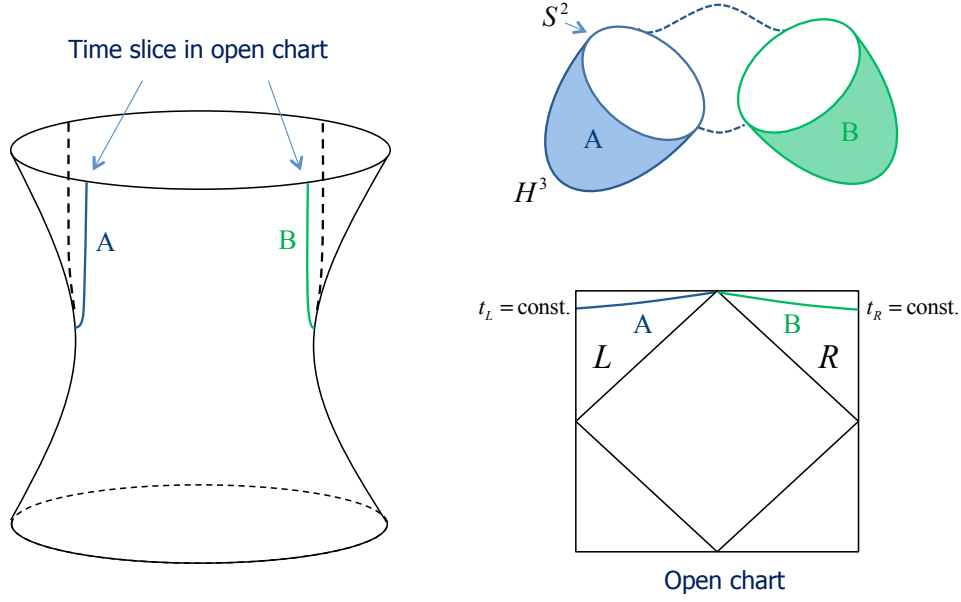


Figure 1: De Sitter space and the Penrose diagram.

2.1 Mode functions in the open chart

The open de Sitter space is studied in detail in [10]. In Figure 1, the de Sitter space and the Penrose diagram is depicted¹. We consider a free scalar field of mass m in de Sitter space with the action given by

$$S = \int d^4x \sqrt{-g} \left[-\frac{1}{2} g^{\mu\nu} \partial_\mu \phi \partial_\nu \phi - \frac{m^2}{2} \phi^2 \right]. \quad (2.1)$$

The metric in each region R and L may be obtained by analytic continuation from an Euclidean four-sphere metric and expressed, respectively, as

$$\begin{aligned} ds_R^2 &= H^{-2} \left[-dt_R^2 + \sinh^2 t_R (dr_R^2 + \sinh^2 r_R d\Omega^2) \right], \\ ds_L^2 &= H^{-2} \left[-dt_L^2 + \sinh^2 t_L (dr_L^2 + \sinh^2 r_L d\Omega^2) \right], \end{aligned} \quad (2.2)$$

where $d\Omega^2$ is the metric on the two-sphere. Since the R and L regions are completely symmetric, if we perform the separation of variables

$$\phi = \frac{H}{\sinh t} \chi_p(t) Y_{p\ell m}(r, \Omega), \quad (2.3)$$

the equations of motion for χ_p and $Y_{p\ell m}$ in the R or L regions are found to be in common

$$\left[\frac{\partial^2}{\partial t^2} + 3 \coth t \frac{\partial}{\partial t} + \frac{1+p^2}{\sinh^2 t} + \frac{m^2}{H^2} \right] \chi_p(t) = 0, \quad (2.4)$$

$$\left[\frac{\partial^2}{\partial r^2} + 2 \coth r \frac{\partial}{\partial r} - \frac{1}{\sinh^2 r} \mathbf{L}^2 \right] Y_{p\ell m}(r, \Omega) = -(1+p^2) Y_{p\ell m}(r, \Omega), \quad (2.5)$$

¹The point between L and R regions is a part of the timelike infinity where infinite volume exists. This gives rise to the presence of the supercurvature modes for a scalar field with sufficiently small mass [10]. In this paper, we do not consider the supercurvature modes.

where $(t, r) = (t_R, r_R)$ or (t_L, r_L) , \mathbf{L}^2 is the Laplacian operator on the unit two-sphere, and $Y_{p\ell m}$ are harmonic functions on the three-dimensional hyperbolic space. We consider the positive frequency mode functions corresponding to the Euclidean vacuum (the Bunch-Davies vacuum [16, 17, 18]), because it is natural that the initial state is the de Sitter invariant vacuum. They are found explicitly in [10] and the time dependent part of $\chi_p(t)$ is given by

$$\chi_{p,\sigma}(t) = \begin{cases} \frac{1}{2 \sinh \pi p} \left(\frac{e^{\pi p - i\sigma} e^{-i\pi\nu}}{\Gamma(\nu + ip + 1/2)} P_{\nu-1/2}^{ip}(\cosh t_R) - \frac{e^{-\pi p - i\sigma} e^{-i\pi\nu}}{\Gamma(\nu - ip + 1/2)} P_{\nu-1/2}^{-ip}(\cosh t_R) \right), \\ \frac{\sigma}{2 \sinh \pi p} \left(\frac{e^{\pi p - i\sigma} e^{-i\pi\nu}}{\Gamma(\nu + ip + 1/2)} P_{\nu-1/2}^{ip}(\cosh t_L) - \frac{e^{-\pi p - i\sigma} e^{-i\pi\nu}}{\Gamma(\nu - ip + 1/2)} P_{\nu-1/2}^{-ip}(\cosh t_L) \right), \end{cases} \quad (2.6)$$

where $P_{\nu-1/2}^{\pm ip}$ are the associated Legendre functions, and the index σ takes the values ± 1 and distinguishes two independent solutions for each region. We have defined a parameter

$$\nu = \sqrt{\frac{9}{4} - \frac{m^2}{H^2}}. \quad (2.7)$$

The above is a solution supported both on the R and L regions. The factor $e^{-\pi p}$ in the above solutions comes from the requirement of analyticity in the Euclidean hemisphere which selects the Bunch-Davies vacuum.

We expand the field in terms of the creation and annihilation operators,

$$\hat{\phi}(t, r, \Omega) = \int dp \sum_{\sigma, \ell, m} \left[a_{\sigma p \ell m} u_{\sigma p \ell m}(t, r, \Omega) + a_{\sigma p \ell m}^\dagger u_{\sigma p \ell m}^*(t, r, \Omega) \right], \quad (2.8)$$

where $a_{\sigma p \ell m}$ satisfies $a_{\sigma p \ell m} |\text{BD}\rangle = 0$. The mode function $u_{\sigma p \ell m}(t, r, \Omega)$ representing the Bunch-Davies vacuum is

$$u_{\sigma p \ell m} = \frac{H}{\sinh t} \chi_{p,\sigma}(t) Y_{p\ell m}(r, \Omega). \quad (2.9)$$

Without loss of generality, we assume the normalization of $Y_{p\ell m}$ is such that $Y_{p\ell m}^* = Y_{p\ell -m}$. Then Eq. (2.8) may be written as

$$\begin{aligned} \hat{\phi}(t, r, \Omega) &= \frac{H}{\sinh t} \int dp \sum_{\sigma, \ell, m} \left[a_{\sigma p \ell m} \chi_{p,\sigma}(t) + a_{\sigma p \ell -m}^\dagger \chi_{p,\sigma}^*(t) \right] Y_{p\ell m}(r, \Omega) \\ &= \int dp \sum_{\ell, m} \phi_{p\ell m}(t) Y_{p\ell m}(r, \Omega), \end{aligned} \quad (2.10)$$

where we introduced a Fourier mode field operator

$$\phi_{p\ell m}(t) \equiv \frac{H}{\sinh t} \sum_{\sigma} \left[a_{\sigma p \ell m} \chi_{p,\sigma}(t) + a_{\sigma p \ell -m}^\dagger \chi_{p,\sigma}^*(t) \right]. \quad (2.11)$$

For convenience, we write the associated Legendre functions of the R and L regions in a simple form $P^{R,L} \equiv P_{\nu-1/2}^{ip}(\cosh t_{R,L})$, $P^{R*,L*} \equiv P_{\nu-1/2}^{-ip}(\cosh t_{R,L})$, then the two lines of Eq. (2.6) may be expressed in one line as

$$\chi^\sigma = N_p^{-1} \sum_{q=R,L} [\alpha_q^\sigma P^q + \beta_q^\sigma P^{q*}] , \quad (2.12)$$

where the index p of $\chi_{p,\sigma}$ is omitted and we defined

$$\alpha_R^\sigma = \frac{e^{\pi p} - i\sigma e^{-i\pi\nu}}{\Gamma(\nu + ip + \frac{1}{2})} , \quad \beta_R^\sigma = -\frac{e^{-\pi p} - i\sigma e^{-i\pi\nu}}{\Gamma(\nu - ip + \frac{1}{2})} , \quad (2.13)$$

$$\alpha_L^\sigma = \sigma \frac{e^{\pi p} - i\sigma e^{-i\pi\nu}}{\Gamma(\nu + ip + \frac{1}{2})} , \quad \beta_L^\sigma = -\sigma \frac{e^{-\pi p} - i\sigma e^{-i\pi\nu}}{\Gamma(\nu - ip + \frac{1}{2})} , \quad (2.14)$$

and N_p is a normalization factor including the $1/(2 \sinh \pi p)$ in Eq. (2.6), given by

$$N_p = \frac{4 \sinh \pi p \sqrt{\cosh \pi p - \sigma \sin \pi \nu}}{\sqrt{\pi} |\Gamma(\nu + ip + 1/2)|} . \quad (2.15)$$

In the above and in what follows, it is understood that the function P^q ($q = R$ or L) defined only in the q region is associated with a step function which is unity in the q region and which vanishes in the opposite region. The complex conjugate of Eq. (2.12) which is necessary in Eq. (2.10) is

$$\chi^{\sigma*} = N_p^{-1} \sum_{q=R,L} [\beta_q^{\sigma*} P^q + \alpha_q^{\sigma*} P^{q*}] . \quad (2.16)$$

If we introduce a 4×4 matrix

$$\chi^I = \begin{pmatrix} \chi^\sigma \\ \chi^{\sigma*} \end{pmatrix} , \quad M^I_J = \begin{pmatrix} \alpha_q^\sigma & \beta_q^\sigma \\ \beta_q^{\sigma*} & \alpha_q^{\sigma*} \end{pmatrix} , \quad P^J = \begin{pmatrix} P^q \\ P^{q*} \end{pmatrix} , \quad (2.17)$$

where $\sigma = \pm 1$, $q = (R, L)$ and the summation is understood when a pair of the same indices appear upstairs and downstairs, then both of Eqs. (2.12) and (2.16) can be accommodated into the simple matrix form,

$$\chi^I = N_p^{-1} M^I_J P^J , \quad (2.18)$$

where the capital indices (I, J) run from 1 to 4. The Fourier mode field operator Eq. (2.11) is then expanded as

$$\phi_{p\ell m}(t) \equiv \phi(t) = \frac{H}{\sinh t} a_I \chi^I = \frac{1}{N_p} \frac{H}{\sinh t} a_I M^I_J P^J , \quad a_I = (a_\sigma, a_\sigma^\dagger) , \quad (2.19)$$

where t stands for a time slice given by $t = t_R$ in the R region and $t = t_L$ in the L region, and in the following the indices p, ℓ, m of $\phi_{p\ell m}(t)$ are omitted for simplicity unless there may be any confusion.

2.2 Spectrum in the L region

Let us calculate the power spectrum, say, in the L region because the R and L regions are completely symmetric. As it is unnecessary to consider the R region, the mode function χ^I given by Eq. (2.18) may be restricted to the L region. This reduces the 4×4 matrix M^I_J to the 4×2 matrix $M^I_{\mathcal{J}}$, where the calligraphic indice \mathcal{J} runs from 1 to 2, and the solution on the L region in Eq. (2.6) is expressed as

$$\chi^I = N_p^{-1} M^I_{\mathcal{J}} P^{\mathcal{J}}, \quad (2.20)$$

where

$$\chi^I = \begin{pmatrix} \chi^\sigma \\ \chi^{\sigma*} \end{pmatrix}, \quad M^I_{\mathcal{J}} = \begin{pmatrix} \alpha^\sigma_L & \beta^\sigma_L \\ \beta^{\sigma*}_L & \alpha^{\sigma*}_L \end{pmatrix}, \quad P^{\mathcal{J}} = \begin{pmatrix} P^L \\ P^{L*} \end{pmatrix}. \quad (2.21)$$

The Fourier mode field operator in Eq. (2.19) is now expressed as

$$\phi(t_L) = \frac{H}{\sinh t_L} a_I \chi^I = \frac{1}{N_p} \frac{H}{\sinh t_L} a_I M^I_{\mathcal{J}} P^{\mathcal{J}}, \quad a_I = (a_\sigma, a^\dagger_\sigma), \quad (2.22)$$

where we used Eq. (2.20).

If we focus on a single mode with indices p, ℓ, m , the mean-square vacuum fluctuation is then computed by using Eq. (2.19) as

$$\begin{aligned} \langle \text{BD} | \phi_{p\ell m}(t_L) \phi^\dagger_{p'\ell' m'}(t_L) | \text{BD} \rangle &= \frac{H^2}{\sinh^2 t_L} \langle \text{BD} | a_I \chi^I (a_J \chi^J)^\dagger | \text{BD} \rangle \\ &= \frac{H^2}{\sinh^2 t_L} \sum_{\sigma=\pm 1} |\chi^\sigma|^2 \delta(p-p') \delta_{\ell\ell'} \delta_{mm'} \\ &\equiv S(p, t_L) \delta(p-p') \delta_{\ell\ell'} \delta_{mm'}. \end{aligned} \quad (2.23)$$

Then the normalized spectrum per unit logarithmic interval of p is given by

$$\mathcal{P}(p, t_L) = \frac{p^3}{2\pi^2} S(p, t_L) = \frac{p^3}{2\pi^2} \frac{H^2}{\sinh^2 t_L} \sum_{\sigma=\pm 1} |\chi^\sigma|^2, \quad (2.24)$$

where $\chi^\sigma = \chi_{p,\sigma}(t_L)$.

2.3 Vacuum fluctuations after horizon exit

In this subsection, we make sure that the amplitude of the vacuum fluctuation is frozen out at the epoch of horizon exit. The time dependence of χ^σ in Eq. (2.20) comes from the associated Legendre functions. So if we write

$$\chi^I = \begin{pmatrix} \chi^\sigma \\ \chi^{\sigma*} \end{pmatrix} = \begin{pmatrix} A^\sigma_L P^L + B^\sigma_L P^{L*} \\ B^{\sigma*}_L P^L + A^{\sigma*}_L P^{L*} \end{pmatrix}, \quad A^\sigma_L \equiv \frac{\alpha^\sigma_L}{N_p}, \quad B^\sigma_L \equiv \frac{\beta^\sigma_L}{N_p}, \quad (2.25)$$

then $|\chi^\sigma|^2$ in the normalized spectrum in Eq. (2.24) is expressed as

$$|\chi^\sigma|^2 = A^\sigma_L B^{\sigma*}_L (P^L)^2 + (|A^\sigma_L|^2 + |B^\sigma_L|^2) P^L P^{L*} + A^{\sigma*}_L B^\sigma_L (P^{L*})^2. \quad (2.26)$$

Since the Legendre functions on superhorizon scale behave as

$$P_{\nu-1/2}^{\pm ip}(\cosh t) \xrightarrow{t \gg 1} \frac{2^{\nu-1/2} \Gamma(\nu)}{\sqrt{\pi} \Gamma(\nu \mp ip + 1/2)} (\cosh t)^{\nu-1/2}, \quad (2.27)$$

we find the time dependence of each combination of the associated Legendre functions in Eq. (2.26) is the same. Then $\sum_{\sigma=\pm 1} |\chi^\sigma|^2$ is given by

$$\begin{aligned} \sum_{\sigma=\pm 1} |\chi^\sigma|^2 &\xrightarrow{t_L \gg 1} \frac{2^{2\nu-1} \Gamma(\nu)^2}{\pi} \sum_{\sigma=\pm 1} \left[\frac{A^\sigma_L B^{\sigma*}_L}{\Gamma(\nu - ip + 1/2)^2} + \frac{|A^\sigma_L|^2 + |B^\sigma_L|^2}{|\Gamma(\nu + ip + 1/2)|^2} + \frac{A^{\sigma*}_L B^\sigma_L}{\Gamma(\nu + ip + 1/2)^2} \right] \\ &\times (\cosh t_L)^{2\nu-1} \\ &\equiv Z (\cosh t_L)^{2\nu-1}, \end{aligned} \quad (2.28)$$

where we defined the time independent part of $\sum_{\sigma=\pm 1} |\chi^\sigma|^2$ by Z .

Plugging Eq. (2.28) into Eq. (2.24), we find the spectrum approaches

$$\mathcal{P}(p, t_L) = \frac{H^2}{\sinh^2 t_L} \sum_{\sigma=\pm 1} |\chi^\sigma|^2 \frac{p^3}{2\pi^2} \xrightarrow{t_L \gg 1} H^2 Z \frac{p^3}{2\pi^2} \frac{(\cosh t_L)^{2\nu-1}}{\sinh^2 t_L}. \quad (2.29)$$

For massless case $\nu = 3/2$, we find the time dependent part becomes

$$\frac{(\cosh t_L)^{2\nu-1}}{\sinh^2 t_L} \xrightarrow{t_L \gg 1} 1. \quad (2.30)$$

Thus, the vacuum fluctuation gets frozen out after horizon exit.

2.4 Wavenumber dependence

We also need to check the behavior of the spectrum at short wavelengths ($p \gg 1$). The spectrum should be the same as the case of a specially flat universe. For the massless scalar field ($\nu = 3/2$), the dominant term in Z of Eq. (2.28) for large p is

$$\sum_{\sigma=\pm 1} \frac{|A^\sigma_L|^2}{|\Gamma(\nu + ip + 1/2)|^2} = \sum_{\sigma=\pm 1} \frac{|\alpha^\sigma_L|^2 / |N_p|^2}{|\Gamma(\nu + ip + 1/2)|^2} \xrightarrow{p \gg 1} \frac{2\pi^2 e^{-2\pi p}}{p^5 |\Gamma(ip)|^4}. \quad (2.31)$$

Then the time independent part of Z at short wavelengths ($p \gg 1$) becomes

$$Z \xrightarrow{p \gg 1} \frac{2^2 \Gamma(3/2)^2}{\pi} \frac{2\pi^2 e^{-2\pi p}}{p^5 |\Gamma(ip)|^4} \sim \frac{1}{2p^3}. \quad (2.32)$$

Thus the spectrum of the massless scalar field after horizon exit is evaluated as

$$\mathcal{P}(p) = H^2 Z \frac{p^3}{2\pi^2} \xrightarrow{p \gg 1} \left(\frac{H}{2\pi} \right)^2. \quad (2.33)$$

This is the well-known result for vacuum fluctuations after horizon exit. The spectrum as a function of p is plotted in Figure 2.

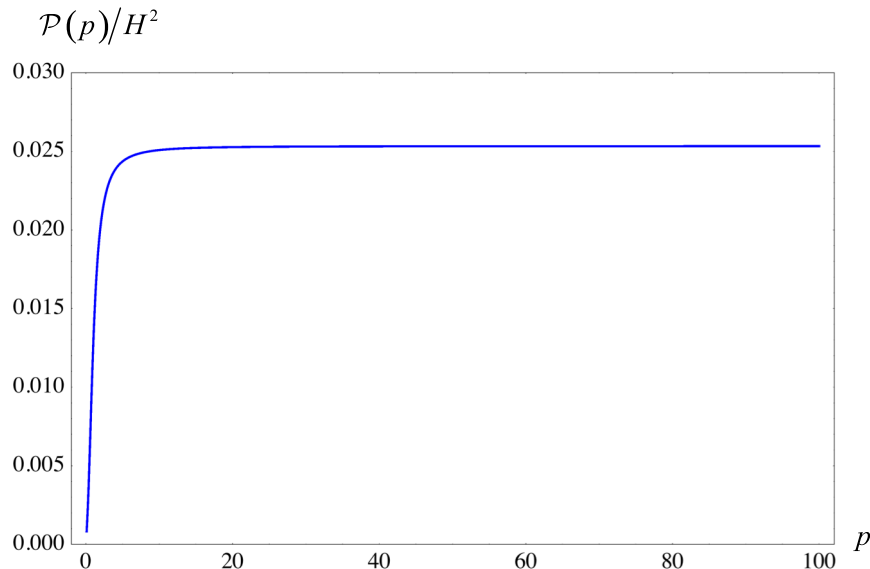


Figure 2: The spectrum of vacuum fluctuations for a massless scalar field as a function of p .

3 Spectrum of quantum fluctuations using the reduced density matrix

In previous section, we discussed the spectrum of vacuum fluctuations by using the field operator expanded in terms of the mode functions defined for the Bunch-Davies vacuum. We next want to explore the spectrum of vacuum fluctuations by using the reduced density matrix derived by Maldacena and Pimentel in [7]. In this section, we first review the formalism to obtain the reduced density matrix and then discuss the spectrum of vacuum fluctuations.

3.1 A review on the reduced density matrix

In order to derive the reduced density matrix in the region L , we need to trace over the degrees of freedom of the region R . To make this procedure practically possible, the reduced density matrix has to be diagonalized. The following is a review on the derivation of the reduced density matrix given in [7].

As we see in Eq. (2.19), the mode function χ^I corresponding to the Bunch-Davies vacuum is a linear combination of the Legendre functions $P^{R,L} = P_{\nu-1/2}^{ip}(\cosh t_{R,L})$, which are proportional to the positive frequency modes in the past in each R or L region. Setting $\tau = \cosh t$, the Legendre functions are known to be normalized as

$$(\tau^2 - 1) \left(\frac{dP^{q*}}{d\tau} P^q - \frac{dP^q}{d\tau} P^{q*} \right) = \frac{2ip}{|\Gamma(1 + ip)|^2}, \quad (3.1)$$

where $q = R$ or L . Thus, the properly normalized positive frequency functions in each R or

L region are given by

$$\varphi^q = N_b^{-1} P^q, \quad N_b = \frac{\sqrt{2p}}{|\Gamma(1+ip)|}. \quad (3.2)$$

Let us introduce φ^I as

$$\varphi^I = \begin{pmatrix} \varphi^q \\ \varphi^{q*} \end{pmatrix}. \quad (3.3)$$

Then this procedure of changing the mode functions from χ^I to φ^I is a Bogoliubov transformation. The Bogoliubov coefficients are then expressed in terms of α and β in the matrix M in Eq. (2.17). So let us introduce new creation and annihilation operators b_I defined such that $b_R|R\rangle = 0$ and $b_L|L\rangle = 0$. Now, with the proper normalization in Eq. (3.2), the original field operator in Eq. (2.19) is expanded in terms of the new operators b_J as

$$\phi(t) = \frac{H}{\sinh t} a_I \chi^I = \frac{H}{\sinh t} b_J \varphi^J, \quad b_J = (b_q, b_q^\dagger), \quad (3.4)$$

where again the capital indices (I, J) run from 1 to 4, $q = (R, L)$, and the repeated indices are summed over. By comparing Eqs. (2.19) and (3.4), the relation between the operators a_I and b_I has to be

$$a_J = N_p N_b^{-1} b_I (M^{-1})^I{}_J, \quad (M^{-1})^I{}_J = \begin{pmatrix} \xi^q{}_\sigma & \delta^q{}_\sigma \\ \delta^{q*}{}_\sigma & \xi^{q*}{}_\sigma \end{pmatrix}, \quad \begin{cases} \xi = (\alpha - \beta \alpha^{*-1} \beta^*)^{-1}, \\ \delta = -\alpha^{-1} \beta \xi^*. \end{cases} \quad (3.5)$$

Note that M^{-1} is not normalized but its determinant is $(|\xi|^2 - |\delta|^2)^{-1/2} = (|\alpha|^2 - |\beta|^2)^{1/2}$, which corresponds to $N_p N_b^{-1}$ in Eq. (3.5). Thus, the Bunch-Davies vacuum can be regarded as a Bogoliubov transformation of the R, L -vacua as

$$|\text{BD}\rangle \propto \exp\left(\frac{1}{2} \sum_{i,j=R,L} m_{ij} b_i^\dagger b_j^\dagger\right) |R\rangle |L\rangle, \quad (3.6)$$

where m_{ij} is a symmetric matrix and the operators b_i satisfy the commutation relation $[b_i, b_j^\dagger] = \delta_{ij}$. Note that the normalization of the Bogoliubov transformation is omitted here for simplicity because it is unnecessary for the derivation of the reduced density matrix, which will be given in Eq. (3.17).

Here we mention a subtlety associated with the fact that the p -mode spectrum is continuous. Since the commutation relation between the p -mode annihilation operator and the p' -mode creation operator is proportional to $\delta(p - p')$, that between the same spectral index $p = p'$ would diverge. To avoid this divergence, we discretize the p -mode spectrum with a width Δp and take the limit $\Delta p \rightarrow 0$ only at the end of computation. This means, for

example, we rescale the operators b_i as $b_i \rightarrow b_i = \sqrt{\Delta p} b_i^{\text{cont}}$, where the index ‘cont’ denotes the operator with the original, continuous spectrum, and the operators b_i and b_j appearing in Eq. (3.6) should be understood as the rescaled ones.

The condition $a_\sigma |\text{BD}\rangle = 0$ determines m_{ij} :

$$m_{ij} = -\delta_{i\sigma}^* (\xi^{-1})_{\sigma j} = e^{i\theta} \frac{\sqrt{2} e^{-p\pi}}{\sqrt{\cosh 2\pi p + \cos 2\pi\nu}} \begin{pmatrix} \cos \pi\nu & i \sinh p\pi \\ i \sinh p\pi & \cos \pi\nu \end{pmatrix}, \quad (3.7)$$

where $e^{i\theta}$ contains all unimportant phase factors for $\nu^2 > 0$.

When the state is written in the form of Eq. (3.6), it is still difficult to trace over the R degrees of freedom because the density matrix $\rho = |\text{BD}\rangle\langle\text{BD}|$ is not diagonal in the $|R\rangle|L\rangle$ basis. Thus, we perform another Bogoliubov transformation further by introducing new operators c_R and c_L

$$c_R = u b_R + v b_R^\dagger, \quad c_L = \bar{u} b_L + \bar{v} b_L^\dagger, \quad (3.8)$$

to obtain the relation

$$|\text{BD}\rangle = N_{\gamma_p}^{-1} \exp\left(\gamma_p c_R^\dagger c_L^\dagger\right) |R'\rangle|L'\rangle. \quad (3.9)$$

Here, the normalizaion $|u|^2 - |v|^2 = 1$ and $|\bar{u}|^2 - |\bar{v}|^2 = 1$ are assumed so that the new operators satisfy the commutation relation $[c_i, c_j^\dagger] = \delta_{ij}$. The normalization factor N_{γ_p} is given by

$$N_{\gamma_p}^2 = \left| \exp\left(\gamma_p c_R^\dagger c_L^\dagger\right) |R'\rangle|L'\rangle \right|^2 = \frac{1}{1 - |\gamma_p|^2}, \quad (3.10)$$

where $|\gamma_p| < 1$ is imposed. Eq. (3.8) is a linear transformation between c_q and b_q , so this Bogoliubov transformation does not mix R and L Hilbert spaces, but the basis vacuum changes from $|R\rangle|L\rangle$ to $|R'\rangle|L'\rangle$.

For later convenience, we introduce a 4×4 matrix form of Eq. (3.8),

$$c_J = b_I G^I{}_J, \quad G^I{}_J = \begin{pmatrix} U_q & V_q^* \\ V_q & U_q^* \end{pmatrix}, \quad c_J = (c_q, c_q^\dagger), \quad (3.11)$$

where $U_q \equiv \text{diag}(u, \bar{u})$, $V_q \equiv \text{diag}(v, \bar{v})$.

The consistency conditions for Eq. (3.9) are

$$c_R |\text{BD}\rangle = \gamma_p c_L^\dagger |\text{BD}\rangle, \quad c_L |\text{BD}\rangle = \gamma_p c_R^\dagger |\text{BD}\rangle. \quad (3.12)$$

If we write $m_{RR} = m_{LL} \equiv \omega$ and $m_{LR} = m_{RL} \equiv \zeta$ in Eq. (3.7), we see that ω is real and ζ is pure imaginary for positive ν^2 . Then inserting Eqs. (3.6) and (3.8) into Eq. (3.12), we find a system of four homogeneous equations

$$\omega u + v - \gamma_p \zeta \bar{v}^* = 0, \quad \zeta u - \gamma_p \bar{u}^* - \gamma_p \omega \bar{v}^* = 0, \quad (3.13)$$

$$\omega \bar{u} + \bar{v} - \gamma_p \zeta v^* = 0, \quad \zeta \bar{u} - \gamma_p u^* - \gamma_p \omega v^* = 0, \quad (3.14)$$

where $\omega^* = \omega$ and $\zeta^* = -\zeta$. We see that setting $v^* = \bar{v}$ and $u^* = \bar{u}$ is possible if γ_p is pure imaginary $\gamma_p^* = -\gamma_p$. This is always possible by adjusting the phase of c_q . Then Eq. (3.14) becomes identical with Eq. (3.13) and the system is reduced to that of two homogeneous equations. We look for such γ_p , keeping the normalization condition $|u|^2 - |v|^2 = 1$ satisfied.

In order to have a non-trivial solution in the system of equations (3.13), γ_p must be

$$\gamma_p = \frac{1}{2\zeta} \left[-\omega^2 + \zeta^2 + 1 - \sqrt{(\omega^2 - \zeta^2 - 1)^2 - 4\zeta^2} \right], \quad (3.15)$$

where we took a minus sign in front of the square root term to satisfy $|\gamma_p| < 1$. Note that γ_p is pure imaginary. Putting the ω and ζ defined in Eq. (3.7) into Eq. (3.15), we get

$$\gamma_p = i \frac{\sqrt{2}}{\sqrt{\cosh 2\pi p + \cos 2\pi\nu} + \sqrt{\cosh 2\pi p + \cos 2\pi\nu + 2}}. \quad (3.16)$$

Now we have the density matrix which enables us to trace over the R degrees of freedom easily. By using Eqs. (3.9) and (3.10), the reduced density matrix is then found to be diagonalized as

$$\rho_L = \text{Tr}_R |\text{BD}\rangle\langle\text{BD}| = (1 - |\gamma_p|^2) \sum_{n=0}^{\infty} |\gamma_p|^{2n} |n; p\ell m\rangle\langle n; p\ell m|, \quad (3.17)$$

where we defined $|n; p\ell m\rangle = 1/\sqrt{n!} (c_L^\dagger)^n |L'\rangle$. Note that this density matrix is for each mode labeled by p, ℓ, m .

3.2 Spectrum of vacuum fluctuations

Now we calculate the mean-square vacuum fluctuations by using the reduced density matrix obtained in Eq. (3.17). Since we traced out the degrees of freedom of the R region, the corresponding field operator has to be defined only in the L region. Also the field operator should act only on $|L'\rangle$ conforming with the reduced density matrix. Then, the Fourier mode field operator should be defined as

$$\begin{aligned} \phi_{Lp\ell m}(t_L) \equiv \phi_L(t_L) &= \frac{1}{N_b} \frac{H}{\sinh t_L} b_{\mathcal{J}} P^{\mathcal{J}} = \frac{1}{N_b} \frac{H}{\sinh t_L} c_{\mathcal{I}} (G^{-1})^{\mathcal{I}}{}_{\mathcal{J}} P^{\mathcal{J}} \\ &\equiv \frac{H}{\sinh t_L} c_{\mathcal{I}} \psi^{\mathcal{I}}, \quad \psi^{\mathcal{I}} = \begin{pmatrix} \psi^L \\ \psi^{L*} \end{pmatrix}, \end{aligned} \quad (3.18)$$

where the calligraphic indices $(\mathcal{I}, \mathcal{J})$ run from 1 to 2, and the matrix is reduced to a 2×2 form:

$$(G^{-1})^{\mathcal{I}}{}_{\mathcal{J}} = \begin{pmatrix} \bar{u}^* & -\bar{v}^* \\ -\bar{v} & \bar{u} \end{pmatrix}, \quad |\bar{u}|^2 - |\bar{v}|^2 = 1. \quad (3.19)$$

Note that we transformed the field operator expanded by b_J in Eq. (3.4) into c_I by using Eq. (3.11)².

Focusing on a single mode with indices p, ℓ, m , the mean-square vacuum fluctuations are then calculated as

$$\text{Tr}_L \rho_L \phi_L \phi_L^\dagger = (1 - |\gamma_p|^2) \sum_{n=0}^{\infty} |\gamma_p|^{2n} \langle n; p\ell m | \phi_L \phi_L^\dagger | n; p\ell m \rangle, \quad (3.20)$$

where $\phi_L = \phi_{Lp\ell m}(t_L)$.

3.3 Spectrum in the L region

We calculate the power spectrum in the L region. The mode function given in Eq. (3.18) is written as

$$\psi^{\mathcal{I}} = N_b^{-1} (G^{-1})^{\mathcal{I}}_{\mathcal{J}} P^{\mathcal{J}} = \begin{pmatrix} \mathcal{A}_L P^L + \mathcal{B}_L P^{L*} \\ \mathcal{B}_L^* P^L + \mathcal{A}_L^* P^{L*} \end{pmatrix}, \quad (3.21)$$

where we defined

$$\mathcal{A}_L = \frac{\bar{u}^*}{N_b}, \quad \mathcal{B}_L = -\frac{\bar{v}^*}{N_b}. \quad (3.22)$$

Here, \bar{u}, \bar{v} are obtained by solving Eq. (3.13) with the solution Eq. (3.16) and imposing the normalization condition $|\bar{u}|^2 - |\bar{v}|^2 = 1$:

$$\bar{u} = \frac{1 - \gamma_p \zeta}{\sqrt{|1 - \gamma_p \zeta|^2 - |\omega|^2}}, \quad \bar{v} = \frac{\omega}{\sqrt{|1 - \gamma_p \zeta|^2 - |\omega|^2}}. \quad (3.23)$$

Here, $\omega = m_{RR} = m_{LL}$ and $\zeta = m_{LR} = m_{RL}$ in Eq. (3.7). Using these we can compute the expectation value for each n -particle state in Eq. (3.20),

$$\begin{aligned} \langle n; p\ell m | \phi_L \phi_L^\dagger | n; p\ell m \rangle &= \frac{1}{n!} \langle L' | (c_L)^n \phi_L \phi_L^\dagger (c_L^\dagger)^n | L' \rangle \\ &= \frac{H^2}{\sinh^2 t_L} \frac{1}{n!} \langle L' | (c_L)^n c_{\mathcal{I}} \psi^{\mathcal{I}} (c_{\mathcal{J}} \psi^{\mathcal{J}})^\dagger (c_L^\dagger)^n | L' \rangle \\ &= \frac{H^2}{\sinh^2 t_L} |\psi^L|^2 (2n + 1), \end{aligned} \quad (3.24)$$

where from the second line to the third line we used

$$\begin{aligned} &\langle L' | (c_L)^n c_{\mathcal{I}} \psi^{\mathcal{I}} (c_{\mathcal{J}} \psi^{\mathcal{J}})^\dagger (c_L^\dagger)^n | L' \rangle \\ &= |\psi^L|^2 n! \langle n; p\ell m | n; p\ell m \rangle + 2 |\psi^L|^2 n^2 (n - 1)! \langle n - 1; p\ell m | n - 1; p\ell m \rangle \\ &= (2n + 1) n! |\psi^L|^2. \end{aligned} \quad (3.25)$$

²The Fourier mode field operator ϕ_L is rescaled in accordance with the discretization of the p -mode spectrum as explained below Eq. (3.6).

Putting Eq. (3.24) into Eq. (3.20), the mean-square vacuum fluctuations for each mode is given by

$$\begin{aligned}\text{Tr}_L \rho_L \phi_L \phi_L^\dagger &= \frac{H^2}{\sinh^2 t_L} |\psi^L|^2 (1 - |\gamma_p|^2) \sum_{n=0}^{\infty} |\gamma_p|^{2n} (2n+1) \\ &= \frac{H^2}{\sinh^2 t_L} |\psi^L|^2 \frac{1 + |\gamma_p|^2}{1 - |\gamma_p|^2}.\end{aligned}\quad (3.26)$$

Note that by comparing with Eq. (2.23), we see the main effect of tracing out the degrees of freedom of the region R seems to come in with the form of $(1 + |\gamma_p|^2)/(1 - |\gamma_p|^2)$. Since $|\gamma_p| \rightarrow 1$ as $p \rightarrow 0$ (for $m = 0$), this extra term enhances the mean-square vacuum fluctuations at long wavelengths ($p \ll 1$). Note also that the mode functions are changed from

$$\chi^I = N_p^{-1} M^I_{\mathcal{J}} P^{\mathcal{J}} \longrightarrow \psi^{\mathcal{I}} = N_b^{-1} (G^{-1})^{\mathcal{I}}_{\mathcal{J}} P^{\mathcal{J}}, \quad (3.27)$$

due to the change from the Bunch-Davies vacuum to L' -vacuum which diagonalized the reduced density matrix as obtained in Eq. (3.17).

3.4 Vacuum fluctuations after horizon exit

As we did in subsection 2.3, let us check the time dependence of $\psi^{\mathcal{I}}$ in Eq. (4.3). From Eq. (3.21), the $|\psi^{\mathcal{I}}|^2$ in the mean-square vacuum fluctuations in Eq. (3.26) is expressed as

$$|\psi^L|^2 = \mathcal{A}_L \mathcal{B}_L^* (P^L)^2 + (|\mathcal{A}_L|^2 + |\mathcal{B}_L|^2) P^L P^{L*} + \mathcal{A}_L^* \mathcal{B}_L (P^{L*})^2. \quad (3.28)$$

Since the Legendre functions on superhorizon scale is the same as in Eq. (2.27), we find the time dependence of this case is the same as Eq. (2.28) and expressed as

$$\begin{aligned}|\psi^L|^2 &\xrightarrow{t_L \gg 1} \frac{2^{2\nu-1} \Gamma(\nu)^2}{\pi} \left[\frac{\mathcal{A}_L \mathcal{B}_L^*}{\Gamma(\nu - ip + 1/2)^2} + \frac{|\mathcal{A}_L|^2 + |\mathcal{B}_L|^2}{|\Gamma(\nu + ip + 1/2)|^2} + \frac{\mathcal{A}_L^* \mathcal{B}_L}{\Gamma(\nu + ip + 1/2)^2} \right] \\ &\times (\cosh t_L)^{2\nu-1} \\ &\equiv \mathcal{Z} (\cosh t_L)^{2\nu-1},\end{aligned}\quad (3.29)$$

where we defined \mathcal{Z} corresponding to Z in Eq. (2.28) for comparison. The spectrum of the vacuum fluctuations corresponding to Eq. (2.24) is now given by

$$\mathcal{P}(p, t_L) = \frac{p^3}{2\pi^2} \text{Tr}_L \rho_L \phi_L \phi_L. \quad (3.30)$$

Plugging Eqs. (3.26) and (3.29) into above, we find the spectrum is found to be

$$\mathcal{P}(p, t_L) = \frac{H^2}{\sinh^2 t_L} |\psi^L|^2 \frac{1 + |\gamma_p|^2}{1 - |\gamma_p|^2} \frac{p^3}{2\pi^2} \xrightarrow{t_L \gg 1} H^2 \mathcal{Z} \frac{1 + |\gamma_p|^2}{1 - |\gamma_p|^2} \frac{p^3}{2\pi^2} \frac{(\cosh t_L)^{2\nu-1}}{\sinh^2 t_L}. \quad (3.31)$$

We see the time dependent part is completely identical with Eq. (2.29). Thus, for massless case ($\nu = 3/2$), the vacuum fluctuation gets frozen after horizon exit in the case of the spectrum using the reduced density matrix as well.

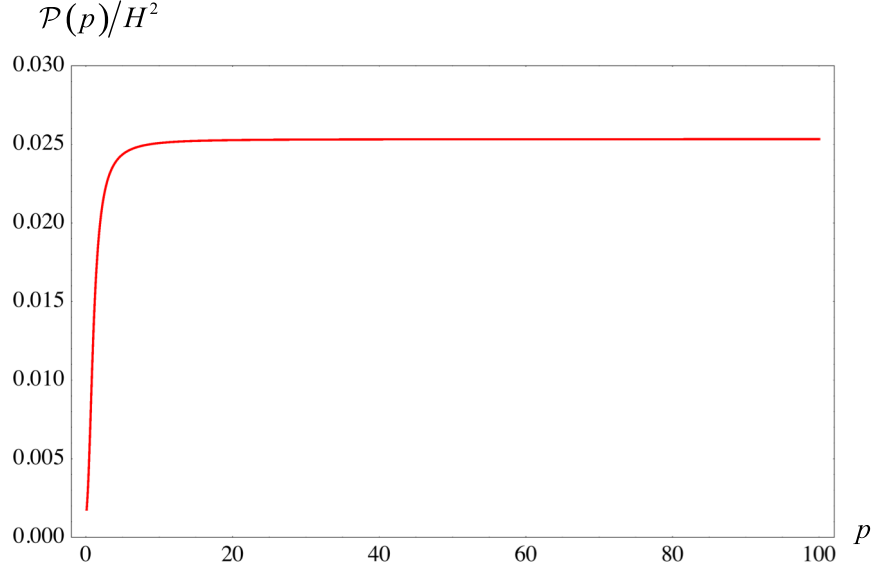


Figure 3: The spectrum as a function of p .

3.5 Wavenumber dependence

Next, let us see the behavior of the power spectrum at short wavelengths ($p \gg 1$) as we did in subsection 2.4. For a massless scalar field ($\nu = 3/2$), the dominant term in \mathcal{Z} of Eq. (3.29) for large p is found to be

$$\frac{|\mathcal{A}_L|^2}{|\Gamma(\nu + ip + 1/2)|^2} = \frac{|\bar{u}|^2/|N_b|^2}{|\Gamma(\nu + ip + 1/2)|^2} \xrightarrow{p \gg 1} \frac{\pi e^{-\pi p}}{2p^4 |\Gamma(ip)|^2}. \quad (3.32)$$

The corresponding case of the Bunch-Davies vacuum is Eq. (2.31). We see the α_L^r/N_p is simply replaced by \bar{u}/N_b , and find that the behavior of \mathcal{Z} is the same as that of Z ,

$$\mathcal{Z} \xrightarrow{p \gg 1} \frac{2^2 \Gamma(3/2)^2}{\pi} \frac{\pi e^{-\pi p}}{2p^4 |\Gamma(ip)|^2} \sim \frac{1}{2p^3}. \quad (3.33)$$

Thus the spectrum of a massless scalar field after horizon exit is evaluated as

$$\mathcal{P}(p) = H^2 \mathcal{Z} \frac{1 + |\gamma_p|^2}{1 - |\gamma_p|^2} \left(\frac{p^3}{2\pi^2} \right) \xrightarrow{p \gg 1} \left(\frac{H}{2\pi} \right)^2. \quad (3.34)$$

We find that the scale invariant spectrum is realized for $p \gg 1$ even after tracing out the degrees of freedom of the region R . We plot the spectrum of the massless scalar field in Eq. (3.34) as a function of p in Figure 3. It is almost identical to Figure 2.

4 Possible observable signatures

So far, we discussed two different spectra given in terms of χ^I and ψ^I . The former correspond to the mode functions for the *entangled* Bunch-Davies vacuum, and the latter to those that

diagonalize the reduced density matrix obtained from the Bunch-Davies vacuum by tracing out the degrees of freedom of the R region. The corresponding states are given by the density matrix $\rho_{\text{BD}} = |\text{BD}\rangle\langle\text{BD}|$ and the reduced density matrix $\rho_L = \text{Tr}_R \rho_{\text{BD}}$, respectively.

The difference between these two states is the observer's point of view when taking the mean-square vacuum fluctuations. For ρ_{BD} , we are supposed to know the entangled state in the region R . On the other hand, for ρ_L , we are supposed to be completely ignorant about the state in the R region. In order to distinguish them, we call ρ_{BD} the “entangled state”, and ρ_L the “mixed state (obtained from the entangled state)”, or just denote them by their relevant mode functions χ^I and $\psi^{\mathcal{I}}$ in the following.

4.1 Non-entangled state

In the subsections 2.4 and 3.5, we showed that both of the entangled state and the mixed state realize the scale invariant spectrum for a massless scalar field at short wavelengths ($p \gg 1$). Now we wonder what would happen to the spectrum if we assume the L region were the whole universe and use the mode function $\varphi^{\mathcal{I}}$ which is defined only in the L region. We call it “non-entangled state”, and denote it by $\varphi^{\mathcal{I}}$.

The relevant mode function for the non-entangled case should be given by Eq. (3.2). That is

$$\varphi^{\mathcal{I}} = \begin{pmatrix} \varphi^L \\ \varphi^{L*} \end{pmatrix} = \frac{1}{N_b} \begin{pmatrix} P^L \\ P^{L*} \end{pmatrix}. \quad (4.1)$$

The spectrum is then defined by

$$\mathcal{P}(p, t_L) = \frac{p^3}{2\pi^2} \langle L | \varphi^L \varphi^L | L \rangle, \quad (4.2)$$

where the Fourier mode field operator is

$$\varphi^L(t_L) = \frac{H}{\sinh t} b_{\mathcal{I}} \varphi^{\mathcal{I}}(t_L), \quad (4.3)$$

and we find the mean-square vacuum fluctuations for each mode

$$\langle L | \varphi^L \varphi^L | L \rangle = \frac{H^2}{\sinh^2 t_L} |\varphi^L|^2 \delta(p - p') \delta_{\ell\ell'} \delta_{mm'}. \quad (4.4)$$

The $|\varphi^L|^2$ becomes a simple form

$$|\varphi^L|^2 = \frac{1}{2p} |\Gamma(1 + ip)|^2 P^L P^{*L} \xrightarrow{t_L \gg 1} \frac{2^{2\nu-1} \Gamma(\nu)^2}{\pi} \frac{|\Gamma(1 + ip)|^2}{|\Gamma(\nu + ip + 1/2)|^2} \frac{1}{2p} (\cosh t_L)^{2\nu-1} \equiv \tilde{\mathcal{Z}} (\cosh t_L)^{2\nu-1}. \quad (4.5)$$

Here, time independent part of $\tilde{\mathcal{Z}}$ at short wavelengths ($p \gg 1$) is evaluated as

$$\tilde{\mathcal{Z}} \xrightarrow{p \gg 1} \frac{2^2 \Gamma(3/2)^2}{\pi} \frac{|\Gamma(1+ip)|^2}{|\Gamma(2+ip)|^2} \frac{1}{2p} \sim \frac{1}{2p^3}. \quad (4.6)$$

The power spectrum becomes

$$\mathcal{P}(p) = H^2 \tilde{\mathcal{Z}} \frac{p^3}{2\pi^2} \xrightarrow{p \gg 1} \left(\frac{H}{2\pi} \right)^2. \quad (4.7)$$

Thus, for $p \gg 1$, we get the flat spectrum of vacuum fluctuations for a massless scalar field even for the non-entangled state. This means that we cannot distinguish which state is valid for our universe as far as we focus on the short wavelength region of the spectrum. So let us examine the behavior at long wavelengths after the horizon exit.

4.2 Spectra at long wavelengths

In order to see the behavior at long wavelengths, we take the limit $p \ll 1$ and expand the expressions for the spectra in p . For $\varphi^{\mathcal{I}}$ and χ^I , we expand $\tilde{\mathcal{Z}}$ in Eq. (4.5) and Z in Eq. (2.28), respectively. Then we find the p dependence at leading order is given by

$$\mathcal{P}(p) \xrightarrow[p \ll 1]{t_L \gg 1} \begin{cases} 2^{2\nu-1} \Gamma(\nu)^2 \pi^{-1} |\Gamma(\nu+1/2)|^{-2} \left(\frac{H}{2\pi} \right)^2 p^2 & \text{for } \varphi^{\mathcal{I}}, \\ 2^{2\nu-1} \Gamma(\nu)^2 |\Gamma(\nu+1/2)|^{-2} \left(\frac{H}{2\pi} \right)^2 p^3 & \text{for } \chi^I. \end{cases} \quad (4.8)$$

In the case of $\psi^{\mathcal{I}}$, we expand \mathcal{Z} in Eq. (3.29) to obtain

$$\begin{aligned} \mathcal{P}(p) \xrightarrow[p \ll 1]{t_L \gg 1} & 2^{2\nu-1} \Gamma(\nu)^2 \sqrt{2} \pi^{-2} |\Gamma(\nu+1/2)|^{-2} |\cos \pi \nu| \left(\sqrt{1 + \cos 2\pi \nu} + \sqrt{3 + \cos 2\pi \nu} \right) \\ & \times \frac{(\sqrt{1 + \cos 2\pi \nu} + \sqrt{3 + \cos 2\pi \nu})^2 + 2}{(\sqrt{1 + \cos 2\pi \nu} + \sqrt{3 + \cos 2\pi \nu})^2 - 2} \left(\frac{H}{2\pi} \right)^2 p \quad \text{for } \psi^{\mathcal{I}}. \end{aligned} \quad (4.9)$$

We are interested in the case of small mass ($|\nu - 3/2| \ll 1$). Taking this limit, we see that the spectrum for $\psi^{\mathcal{I}}$ decreases most slowly as $p \rightarrow 0$. The spectra at long wavelengths are plotted in Figure 4, where we take $m^2 = H^2/10$. The spectra for the entangled state (χ^I) and the mixed state ($\psi^{\mathcal{I}}$) are the blue line and the red line, respectively. The green line is the spectrum for the non-entangled state ($\varphi^{\mathcal{I}}$). The non-entangled state seems to give the most suppressed spectrum at $p \ll 1$. But if we use the logarithmic plots (right panel) we find the result is consistent with the analysis of the p dependence in Eqs. (4.8) and (4.9).

Around the curvature scale of the open universe ($p \sim 1$), we find that the green line starts to deviate from other two lines as $p \rightarrow 0$. This point tells us if the regions R and L are entangled or not. Around 5 times of the curvature scale of the open universe ($p \sim 0.2$), the red and blue lines start to bifurcate. This tells us which state among the entangled state and the mixed state is appropriate for our universe.

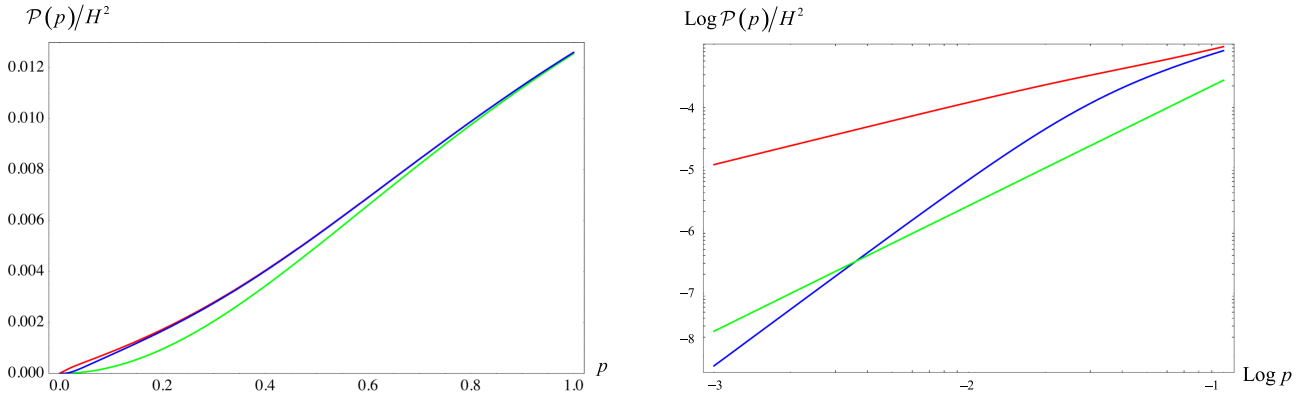


Figure 4: The spectrum at long wavelengths (Left) and the logarithmic plot at very long wavelengths (Right). The red line is for $\psi^{\mathcal{I}}$, the blue line is for $\chi^{\mathcal{I}}$, and the green is for $\varphi^{\mathcal{I}}$.

5 Summary and discussion

We investigated the spectrum of vacuum fluctuations with quantum entanglement in de Sitter space by using the reduced density matrix obtained by Maldacena and Pimentel in [7]. We formulated the mean-square vacuum fluctuations by introducing the two open charts, L and R , which are entangled. We found that the effect of tracing out the degrees of freedom of the R region comes in to the mean-square of vacuum fluctuations and enhances it on scales larger than the curvature radius. On the other hand, on small scales, the spectrum of vacuum fluctuations of a massless scalar field is found to be scale invariant, and completely indistinguishable from the pure Bunch-Davies (hence highly entangled) case.

We also considered a fictitious case in which we assume the L region were the whole universe. In this case, with respect to a natural vacuum state defined in the L region, the scale invariant spectrum is also realized on small scales. Thus it turned out that we cannot distinguish which state is valid for our universe among the entangled state ($\chi^{\mathcal{I}}$), the mixed state from the entangled state ($\psi^{\mathcal{I}}$) and non-entangled state ($\varphi^{\mathcal{I}}$), as long as we focus on the spectrum on small scales.

On the other hand, the spectrum for each of these three cases is found to be different from each other on large scales comparable to or greater than the curvature radius.

We found that the spectra for the entangled and mixed states tend to be enhanced compared to the non-entangled state on scales comparable to the curvature radius. If we go further to scales much larger than the curvature radius, there appears a difference between the entangled state and mixed state. The spectrum for the mixed state is enhanced substantially relative to the entangled state. Since we can use these differences to distinguish those three states, they seem to be relevant (and hopefully observationally testable) in the context of open inflation.

Now let us consider why the difference appeared in the spectra between the entangled

and mixed states. In general, if we consider two subsystems A and B that form a state $|\Psi\rangle$, the expectation value of a physical quantity \mathcal{O} is expressed by using the density matrix $\rho = |\Psi\rangle\langle\Psi|$ as

$$\text{Tr}\rho\mathcal{O} = \sum_{\alpha,\beta} \langle\alpha, \beta|\Psi\rangle\langle\Psi|\mathcal{O}|\alpha, \beta\rangle = \langle\Psi|\mathcal{O}|\Psi\rangle. \quad (5.1)$$

If \mathcal{O} depends only on A , that is, \mathcal{O}_A :

$$\langle\alpha', \beta'|\mathcal{O}|\alpha, \beta\rangle = \langle\alpha|\mathcal{O}_A|\alpha'\rangle\delta_{\beta\beta'}, \quad (5.2)$$

then Eq. (5.1) becomes

$$\begin{aligned} \text{Tr}\rho\mathcal{O}_A &= \sum_{\alpha,\beta} \sum_{\alpha',\beta'} \langle\alpha, \beta|\Psi\rangle\langle\Psi|\alpha', \beta'\rangle\langle\alpha', \beta'|\mathcal{O}_A|\alpha, \beta\rangle = \sum_{\alpha,\beta} \sum_{\alpha'} \langle\alpha, \beta|\Psi\rangle\langle\Psi|\alpha', \beta\rangle\langle\alpha'|\mathcal{O}_A|\alpha\rangle \\ &= \text{Tr}\rho_A\mathcal{O}_A, \end{aligned} \quad (5.3)$$

where

$$\rho_A \equiv \text{Tr}_B\rho = \sum_{\alpha,\alpha'} |\alpha\rangle \left(\sum_{\beta} \langle\alpha, \beta|\Psi\rangle\langle\Psi|\alpha', \beta\rangle \right) \langle\alpha'|. \quad (5.4)$$

Thus, the expectation value $\text{Tr}\rho\mathcal{O}$ is equal to $\text{Tr}\rho_A\mathcal{O}_A$ if \mathcal{O} does not depend on B . In other words, for an operator with the property $\mathcal{O} = \mathcal{O}_A$, the expectation value should agree with each other.

Based on this general argument, we may understand the reason why the spectra for the entangled state and the mixed state from the entangled state become different on large scale ($p \rightarrow 0$). We see that the creation and annihilation operators a_J include the operators on both sides, $b_J = (b_q, b_q^\dagger)$ ($q = R, L$), as in Eq. (3.5). This means that the field operator $\phi(t)$ naturally involves operators on both sides even if the time slice t is restricted to the L region. On the other hand, after tracing out the degrees of freedom of the R region, the mixed state ($\psi^{\mathcal{I}}$) is described by the creation and annihilation operators defined only in the L region. That is, the field operator $\phi_L(t)$ is defined only in the L region. Thus apparently $\phi(t) \neq \phi_L(t)$, implying that the above general argument does not hold because $\mathcal{O} \neq \mathcal{O}_A$.

Finally, we mention that it would be easy to extend our analysis to the case of gravitons. Another direction is to consider interactions. The formalism we developed in this paper is at tree level. It would be interesting to consider the loop corrections and see how they affect the result. They might enhance the effect of the entanglement on small scales because of the coupling between long and short wavelengths [19].

Acknowledgments

I would like to thank Jiro Soda and Misao Sasaki for fruitful discussions, and for helpful suggestions and comments. I would also like to thank Alex Vilenkin and Jaume Garriga for careful reading of the draft, and for very useful suggestions and comments. This work was supported in part by funding from the University Research Council of the University of Cape Town.

References

- [1] S. R. Coleman and F. De Luccia, Phys. Rev. D **21**, 3305 (1980).
- [2] J. Garriga, S. Kanno, M. Sasaki, J. Soda and A. Vilenkin, JCAP **1212**, 006 (2012) [arXiv:1208.1335 [hep-th]].
- [3] J. Garriga, S. Kanno and T. Tanaka, JCAP **1306**, 034 (2013) [arXiv:1304.6681 [hep-th]].
- [4] M. B. Fröb, J. Garriga, S. Kanno, M. Sasaki, J. Soda, T. Tanaka and A. Vilenkin, JCAP **1404**, 009 (2014) [arXiv:1401.4137 [hep-th]].
- [5] S. Ryu and T. Takayanagi, Phys. Rev. Lett. **96**, 181602 (2006) [hep-th/0603001].
- [6] T. Takayanagi, Class. Quant. Grav. **29**, 153001 (2012) [arXiv:1204.2450 [gr-qc]].
- [7] J. Maldacena and G. L. Pimentel, JHEP **1302**, 038 (2013) [arXiv:1210.7244 [hep-th]].
- [8] S. Kanno, J. Murugan, J. P. Shock and J. Soda, arXiv:1404.6815 [hep-th].
- [9] N. Iizuka, T. Noumi and N. Ogawa, arXiv:1404.7487 [hep-th].
- [10] M. Sasaki, T. Tanaka and K. Yamamoto, Phys. Rev. D **51**, 2979 (1995) [gr-qc/9412025].
- [11] M. Bucher, A. S. Goldhaber and N. Turok, Phys. Rev. D **52**, 3314 (1995) [hep-ph/9411206].
- [12] A. D. Linde, Phys. Lett. B **351**, 99 (1995) [hep-th/9503097].
- [13] A. D. Linde and A. Mezhlumian, Phys. Rev. D **52**, 6789 (1995) [astro-ph/9506017].
- [14] J. Garriga, X. Montes, M. Sasaki and T. Tanaka, Nucl. Phys. B **513**, 343 (1998) [astro-ph/9706229].

- [15] J. Garriga, X. Montes, M. Sasaki and T. Tanaka, Nucl. Phys. B **551**, 317 (1999) [astro-ph/9811257].
- [16] T. S. Bunch and P. C. W. Davies, Proc. Roy. Soc. Lond. A **360**, 117 (1978).
- [17] N. A. Chernikov and E. A. Tagirov, Annales Poincare Phys. Theor. A **9**, 109 (1968).
- [18] J. B. Hartle and S. W. Hawking, Phys. Rev. D **28**, 2960 (1983).
- [19] T. Tanaka and Y. Urakawa, Class. Quant. Grav. **30**, 233001 (2013) [arXiv:1306.4461 [hep-th]].